

# Chapter 2. Physics of InAlAs/InGaAs Heterostructure Field-Effect Transistors

## Academic and Research Staff

Professor Jesús A. del Alamo

## Graduate Students

Mark H. Somerville

## Undergraduate Students

Alexander N. Ernst

## Technical and Support Staff

Lisa B. Zeidenberg

## 2.1 Introduction

### Sponsors

Joint Services Electronics Program  
Contract DAAH04-95-1-0038  
Texas Instruments

The goal of this project is to support the development of InAlAs/InGaAs heterostructure field-effect transistors suitable for millimeter-wave high-power applications. This is a key component missing for millimeter-wave radar and communication systems.

Our team has been involved in research on high-power InAlAs/InGaAs heterostructure field-effect transistors for several years. Key contributions in the past have been the demonstration that the use of AlAs-rich InAlAs pseudoinsulators substantially improves the breakdown voltage<sup>1</sup> and demonstration of selective recessed-mesa sidewall isolation to reduce gate leakage current.<sup>2</sup> We also

recently identified the detailed physical mechanisms responsible for breakdown in InAlAs/InGaAs HFETs<sup>3</sup> and the kink effect.<sup>4</sup>

In the last period of performance, we have built the first predictive model for the off-state breakdown voltage in InAlAs/InGaAs and AlGaAs/InGaAs power high-electron mobility transistors (HEMTs). The proposed model suggests that electron tunneling from the gate edge and not impact ionization, is responsible for off-state breakdown in these devices. The model indicates that the crucial variables in determining the off-state breakdown voltage of power HEMTs are (1) the sheet carrier concentration in the extrinsic gate-drain region and (2) the gate Schottky barrier height. Other design parameters have only secondary impact on the breakdown voltage for realistic device designs. Our new model will enable first-pass success in the design of future millimeter-wave systems based on these devices.

<sup>1</sup> S.R. Bahl, W.J. Azzam, and J.A. del Alamo, "Strained-Insulator In<sub>x</sub>Al<sub>1-x</sub>As/n-In<sub>0.53</sub>Ga<sub>0.47</sub> Heterostructure Field-Effect Transistors," *IEEE Trans. Electron. Dev.* 38: 1986 (1991).

<sup>2</sup> S.R. Bahl and J.A. del Alamo, "Elimination of Mesa-Sidewall Gate-Leakage in InAlAs/InGaAs Heterostructures by Selective Sidewall Recessing," *IEEE Electron. Dev. Lett.* 13: 195 (1992).

<sup>3</sup> S.R. Bahl and J.A. del Alamo, "Physics of Breakdown in InAlAs/n-InGaAs Heterostructure Field-Effect Transistors," *IEEE Trans. Electron. Dev.* 41: 2268 (1994); S.R. Bahl, J.A. del Alamo, J. Dickmann, and S. Schildberg, "Off-State Breakdown in InAlAs/InGaAs MODFETs," *IEEE Trans. Electron. Dev.* 42: 15 (1995).

<sup>4</sup> M.H. Somerville, J.A. del Alamo, and W.E. Hoke, "A New Physical Model for the Kink Effect on InAlAs/InGaAs HEMTs," *International Electronic Devices Meeting*, Washington, D.C., December 10-13, 1995, p. 201.

## 2.2 A Model for Tunneling-Limited Breakdown in High-Power HEMTs

Although initially targeted at low-noise applications, InAlAs/InGaAs and AlGaAs/InGaAs high-electron mobility transistors (HEMTs) are enjoying significant success in microwave and millimeter wave power applications.<sup>5</sup> This has been accompanied by major strides towards the improvement of off-state breakdown in these devices through the use of novel recess, cap, channel, and insulator designs.<sup>6</sup>

As impressive as recent reports of breakdown voltage improvement are, work in this area has been largely empirical and has relied primarily on know-how gained from models of MESFET breakdown.<sup>7</sup> MESFET models are based upon the assumption that impact ionization determines the off-state breakdown voltage. The portability of these models should be questionable just on the grounds that modern power HEMT geometries differ substantially from MESFETs.

Recently several authors have suggested that impact ionization alone cannot explain the off-state breakdown behavior of HEMTs. Bahl et al. have proposed a two-step mechanism in which electrons injected from the gate initiate impact ionization in the channel.<sup>8</sup> Crosnier et al. appeal to tunneling in off-state as well.<sup>9</sup> Nonetheless, no *predictive* model currently exists for the off-state breakdown voltage of HEMTs. This hampers first-pass design success. Motivated by mounting experimental evidence that off-state breakdown is largely determined by tunneling and/or thermionic field emission,<sup>10</sup> and not simply impact ionization, we propose a new model for tunneling-limited breakdown in power HEMTs.

In figure 1 we plot the results of several temperature-dependent studies of HEMT breakdown voltage (BV) in the AlGaAs/InGaAs system and the InAlAs/InGaAs system.<sup>11</sup> Also plotted are recently reported results for a modern GaAs MESFET design. Strikingly, *all* these devices exhibit BV with temperature coefficients close to or less than zero. Of course, if impact ionization were the dominant mechanism, we would expect a positive temper-

- 
- <sup>5</sup> J.J. Brown, J.A. Pustl, M. Hu, A.E. Schmitz, D.P. Docter, J.B. Shealy, M.G. Case, M.A. Thompson, and L.D. Nguyen, "High-Efficiency GaAs-based pHEMT C-band Power Amplifier," *IEEE Micro. Guided Wave Lett.* 6(2): 91 (1996); M. Aust, H. Wang, M. Biedenbender, R. Lai, D.C. Streit, P.H. Liu, G.S. Dow, and B.R. Allen, "A 94-GHz Monolithic Power Amplifier using 0.1  $\mu\text{m}$  Gate GaAs-based HEMT MMIC Production Process Technology," *IEEE Micr. Guided Wave Lett.* 5(1): 12 (1995); S.W. Chen, P.M. Smith, S.J. Liu, W.F. Kopp, and T.J. Rogers, "A 60-GHz High Efficiency Monolithic Power Amplifier Using 0.1  $\mu\text{m}$  pHEMTs," *IEEE Micro. Guided Wave Lett.* 5(6): 201 (1995); P.M. Smith, S.J. Liu, M.Y. Kao, P. Ho, S.C. Wang, K.H. Duh, S.T. Fu, and P.C. Chao, "W-band High Efficiency InP-based Power HEMT with 600 GHz  $f_{\text{max}}$ ," *IEEE Micro. Guided Wave Lett.* 5(7): 230 (1995).
- <sup>6</sup> J.C. Huang, G.S. Jackson, S. Shanfield, A. Platzker, P.K. Saledas, and C. Weichert, "An AlGaAs/InGaAs pHEMT with Improved Breakdown Voltage for X- and Ku-band Power Applications," *IEEE Trans. Micro. Theory Tech.* 41 (5): 752 (1993); K.Y. Hur, R.A. McTaggart, B.W. LeBlanc, W.E. Hoke, A.B. Miller, T.E. Kazior, and L.M. Aucoin, "Double Recessed AlInAs/GaInAs/InP HEMTs with High Breakdown Voltages," *IEEE GaAs IC Symp.* 101 (1995); S.R. Bahl and J.A. del Alamo, "Breakdown Voltage Enhancement from Channel Quantization in InAlAs/n-InGaAs HFETs," *IEEE Elect. Dev. Lett.* 13(2): 123 (1992); G. Meneghesso, M. Matloubian, J. Brown, T. Liu, C. Canali, A. Mion, A. Neviani, and E. Zanoni, "Open Channel Impact Ionization Effects in InP-based HEMTs and Their Dependence on Channel Quantization and Temperature," *54th Device Research Conference, Santa Barbara, California, 1996*, p.138.
- <sup>7</sup> S.H. Wemple, W.C. Niehaus, H.M. Cox, J.V. Dilorenzo, and W.O. Schlosser, "Control of Gate-Drain Avalanche in GaAs MESFETs," *IEEE Trans. Elect. Dev.* ED-27(6): 1013 (1980); C. Chang and D.S. Day, "An Analytic Solution of the Two-dimensional Poisson Equation and a Model of Gate Current and Breakdown Voltage for Reverse Gate-drain Bias in GaAs MESFETs," *Solid State Electron.* 32(11): 971 (1989); W.R. Frensley, "Power-limiting Breakdown Effects in GaAs MESFETs," *IEEE Trans. Electron. Dev.* ED-28(8): 962 (1981).
- <sup>8</sup> S.R. Bahl, J.A. del Alamo, J. Dickmann, and S. Schildberg, "Off-State Breakdown in InAlAs/InGaAs MODFETs," *IEEE Trans. Electron. Dev.* 42: 15 (1995).
- <sup>9</sup> Y. Crosnier, "Power FET Families, Capabilities and Limitations from 1 to 100 GHz," *24th Eur. Micro. Conf.* 1: 88 (1994).
- <sup>10</sup> S.R. Bahl, J.A. del Alamo, J. Dickmann, and S. Schildberg, "Off-State Breakdown in InAlAs/InGaAs MODFETs," *IEEE Trans. Electron. Dev.* 42: 15 (1995); M.H. Somerville, J.A. del Alamo, and P. Saunier, "Off-state Breakdown in Power pHEMTs: The Impact of the Source," *Fifty-fourth Device Research Conference*, 1996, p.140.
- <sup>11</sup> S.R. Bahl, J.A. del Alamo, J. Dickmann, and S. Schildberg, "Off-State Breakdown in InAlAs/InGaAs MODFETs," *IEEE Trans. Electron. Dev.* 42: 15 (1995); M.H. Somerville, J.A. del Alamo, and P. Saunier, "Off-state Breakdown in Power pHEMTs: The Impact of the Source," *54th Device Research Conference*, 1996, p.140.; C. Tedesco, E. Zanoni, C. Canali, S. Bigliardi, M. Manfredi, D.C. Streit, and W.T. Anderson, "Impact Ionization and Light Emission in High-power Pseudomorphic AlGaAs/InGaAs HEMTs," *IEEE Trans. Electron. Dev.* 40(7): 1211 (1993); C. Gaquiere, B. Bonte, D. Theron, Y. Crosnier, P. Arsene-Henri, and T. Pacou, "Breakdown Analysis of an Asymmetrical Double Recessed Power MESFET," *IEEE Trans. Electron. Dev.* 42(2): 209 (1995).

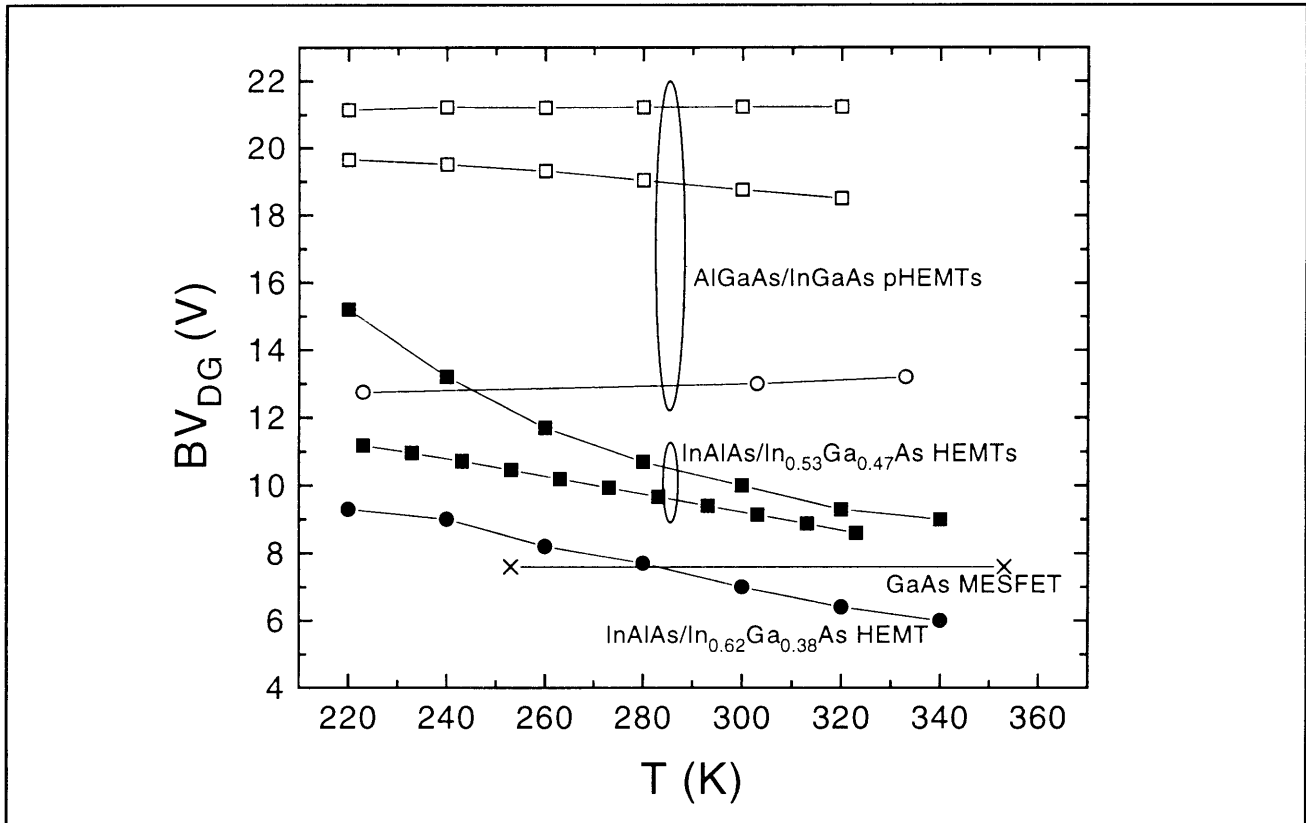


**Figure 1.** Temperature dependence of  $BV_{DG}$  in a variety of HEMT and MESFET structures.  $BV_{DG}$  almost uniformly exhibits temperature dependence close to or less than zero. This implies that tunneling and thermionic field emission are the dominant breakdown mechanisms.

ature coefficient, for, although there is some discussion of the temperature dependence of impact ionization in InGaAs on InP, the suppression of impact ionization with increasing temperature in the GaAs system is well-known.<sup>12</sup>

These results suggest that while impact ionization may play some role in the BV mechanism, BV is dominated by tunneling or thermally-assisted tunneling. Gate-current reverse-bias barrier height extractions offer confirmation that a thermally assisted tunneling mechanism is responsible for off-state breakdown. Both in the AlGaAs/InGaAs system and in the InAlAs/InGaAs system, such extractions yield low activation energies ( $< 0.2$  eV) which drop as  $V_{DG}$  increases.<sup>10</sup>

To understand how tunneling can limit BV, we first examine the geometry of a typical power HEMT (figure 2). If indeed tunneling is the dominant mechanism, determination of BV boils down to an electrostatics problem: for a given  $V_{DG}$ , what is the

magnitude of the field beneath the drain end of the gate? Once this field and the Schottky barrier height ( $\phi_B$ ) are known, determination of tunneling (or thermionic field emission) current is straightforward.

In typical power HEMT designs, two physical observations allow us to construct a simple model for the electrostatics. First, as  $V_{DG}$  is increased, a depletion region of length  $x_D$  opens up in the extrinsic portion of the channel starting from the drain side of the gate; all the depleted charge from this region must be imaged on the gate. Second, in well-designed power HEMTs  $x_D$  is significantly greater than the vertical dimensions  $t_{chan}$  and  $t_{ins}$ . When  $x_D$  is large, the geometry of this problem becomes virtually one-dimensional, so that the field on the drain end of the gate will not depend much on insulator thickness, channel thickness, doping ratio, or gate length. Indeed, the only relevant parameters to determine the field in this picture are  $x_D$  and the

<sup>12</sup> G. Meneghesso, M. Matloubian, J. Brown, T. Liu, C. Canali, A. Mion, A. Neviani, and E. Zanoni, "Open Channel Impact Ionization Effects in InP-based HEMTs and Their Dependence on Channel Quantization and Temperature," *54th Devices Research Conference*, 1996, p.138.

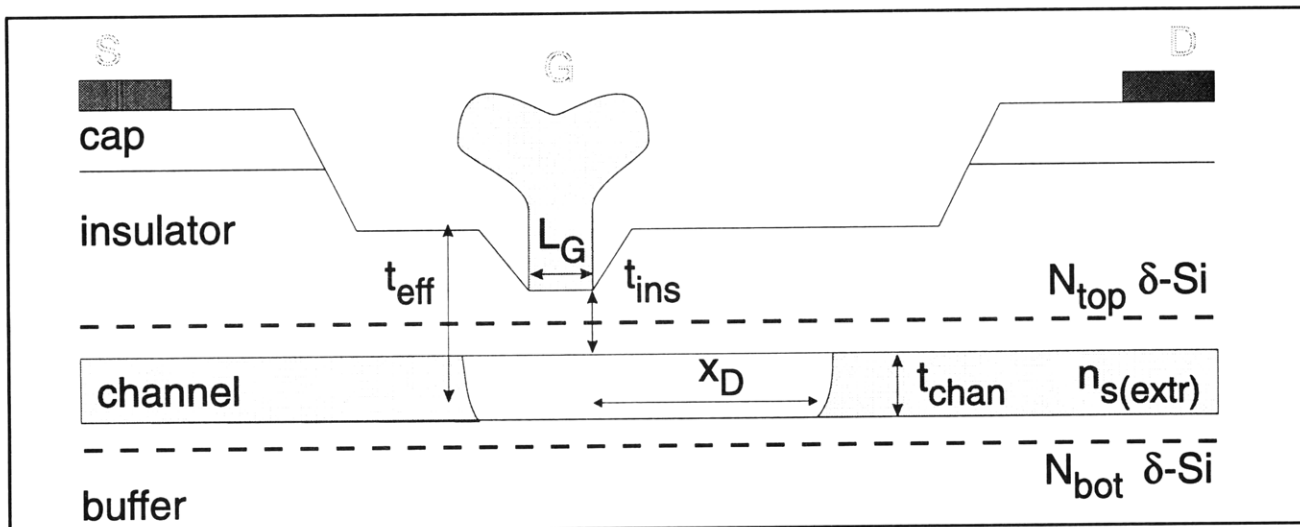


**Figure 2.** Cross-section of a typical power HEMT.  $x_D$  is defined as the length of the drain depletion region measured from the drain edge of the gate;  $n_{s(extr)}$  is the sheet carrier concentration in the extrinsic (wide recess) region; and  $N_{top}$  and  $N_{bot}$  are respectively the top and bottom doping levels.

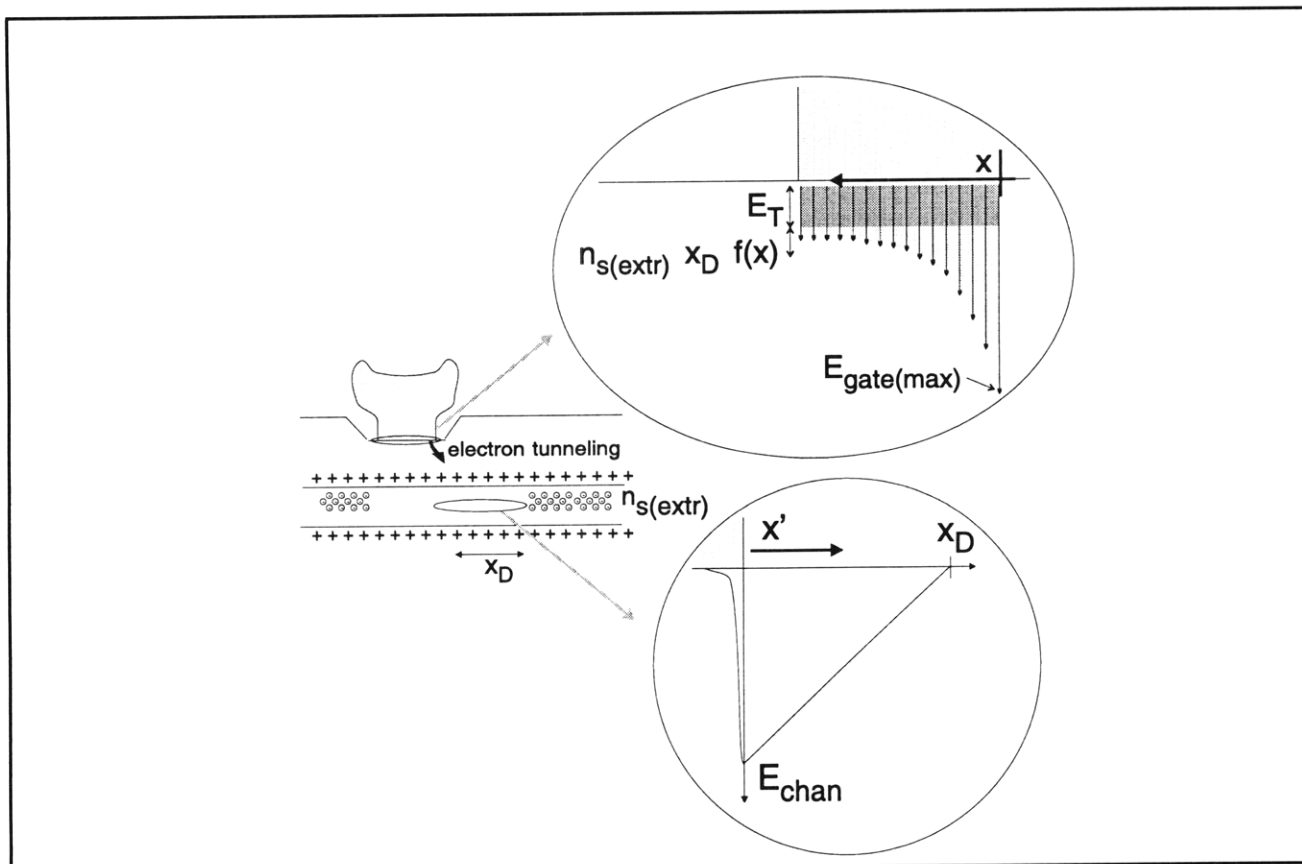


**Figure 3.** Illustration of postulated field profile beneath the gate,  $E_{gate(max)}$ , and in the extrinsic drain,  $E_{chan(max)}$ .  $E_{gate}$  is strongly peaked at the drain end of the gate and obeys a simple functional description that depends only on the carrier concentration in the extrinsic region and the extent of lateral depletion.  $E_{chan}$  has a triangular shape given by a depletion approximation. We define the coordinate  $x$  as the lateral position beneath the gate measured from the gate edge, while the coordinate  $x'$  is the lateral distance within the channel measured from the gate edge towards the drain.

extrinsic sheet carrier concentration ( $n_{s(\text{extr})}$ ). If  $n_{s(\text{extr})}$  is constant over  $x_D$ , the field beneath the gate is proportional to  $x_D$ .

With these physical insights in mind, we propose the simplified field distribution outlined in figure 3: for  $V_{DG}=V_T$ , the field beneath the gate is constant at  $E_T$ ; as  $V_{DG}$  grows, all additional depletion charge is imaged across the gate according to some distribution that is independent of  $x_D$ , so that at any point on the gate the total additional field is proportional to both  $x_D$  and  $n_{s(\text{extr})}$ . We further expect the field beneath the gate to be strongly peaked at the drain end of the gate, reaching a value  $E_{\text{gate(max)}}$ . Finally, in the depleted portion of the drain, the field should have a triangular shape, as the depletion approximation demands. Thus,  $E_{\text{gate(max)}}$  should rise as the square root of  $V_{DG}$ .

The simplifications we propose are borne out by examination of Frensley's MESFET avalanche breakdown model, which solves the field distribution in a simplified (semi-infinite gate) case.<sup>13</sup> The model predicts that when the depletion length is greater than the vertical dimension of the problem, differential changes in  $x_D$  produce a differential increase in field at the gate edge that is independent of  $x_D$  and only weakly dependent on the insulator thickness. Indeed, when  $x_D \geq t_{\text{eff}}$ , we can write the field beneath the gate

$$E_{\text{gate}(x)} \approx \frac{qn_{s(\text{extr})}x_D}{\epsilon_s} \frac{2}{\pi \left(1 + \frac{4x}{\pi t_{\text{eff}}}\right) \sqrt{\pi t_{\text{eff}}x}} + E_T \quad (1)$$

where  $t_{\text{eff}}$  is the location of the centroid of charge (nominally the distance from the surface to the center of the channel), and  $E_T$  the field beneath the gate at threshold. Calculation of  $V_{DG}$  in the  $x_D \geq t_{\text{eff}}$  case becomes relatively simple as well; to first order,

$$V_{DG} - V_T \approx \frac{0.7qn_{s(\text{extr})}x_D^2}{2\epsilon_s t_{\text{eff}}} \quad (2)$$

Equation (2) is then submitted into equation (1) to determine the field-voltage relationship:

$$E_{\text{gate}(x)} - E_T \approx \frac{\sqrt{\frac{2.8qn_{s(\text{extr})}(V_{DG} - V_T)}{\epsilon_s}}}{\pi \left(1 + \frac{4x}{\pi t_{\text{eff}}}\right) \sqrt{\pi x}} \quad (3)$$

Note that as is the case in avalanche models<sup>14</sup> the field near the gate edge (which determines the tunneling current) has virtually no dependence on  $t_{\text{eff}}$ .

Of course, such a model is not entirely appropriate for calculating tunneling current, given that the field diverges at the gate edge. This effect arises from the fact that the transformation does not consider the gate corner accurately. To account for this we cut off the field at some finite distance ( $\sim 70 \text{ \AA}$ ) from the gate corner.<sup>15</sup> Gate current is then calculated easily:

$$I_G = \int_{x_{\text{min}}}^{L_G} \frac{q^2 m_0 E_{\text{gate}(x)}^2}{8\pi \hbar m \phi_B} \exp \left[ \frac{-4\sqrt{2qm} \phi_B^{3/2}}{3\hbar E_{\text{gate}(x)}} \right] dx \quad (4)$$

BV is defined as the value of  $V_{DG}$  that gives rise to a certain value of  $I_G$ , typically 1 mA/mm.

In order to validate this model, we have performed extensive electrostatic simulations of realistic HEMT structures (figure 2) using MEDICI. The values of variable parameters are listed in table 1. From these simulations, we have extracted the magnitude of the field beneath the gate for two bias conditions (figure 4). Also plotted are the field distributions predicted by the model.

<sup>13</sup> W.R. Frensley, "Power-limiting Breakdown Effects in GaAs MESFETs," *IEEE Trans. Elect. Dev.* ED-28(8): 962 (1981).

<sup>14</sup> S.H. Wemple, W.C. Niehaus, H.M. Cox, J.V. Dileo, and W.O. Schlosser, "Control of Gate-Drain Avalanche in GaAs MESFETs," *IEEE Trans. Electron. Dev.* ED-27(6): 1013 (1980); W.R. Frensley, "Power-limiting Breakdown Effects in GaAs MESFETs," *IEEE Trans. Elect. Dev.* ED-28(8): 962 (1981).

<sup>15</sup> H. Muto, H. Kitabayashi, K. Nakanishi, S. Wake, and M. Nakajima, "Simulation of Tunneling Current Due to Enhanced Electric Fields at the Edge of Gate Electrode," *International Conference on Solid State Devices and Materials*, Chiba, Japan, 1993, p.264.

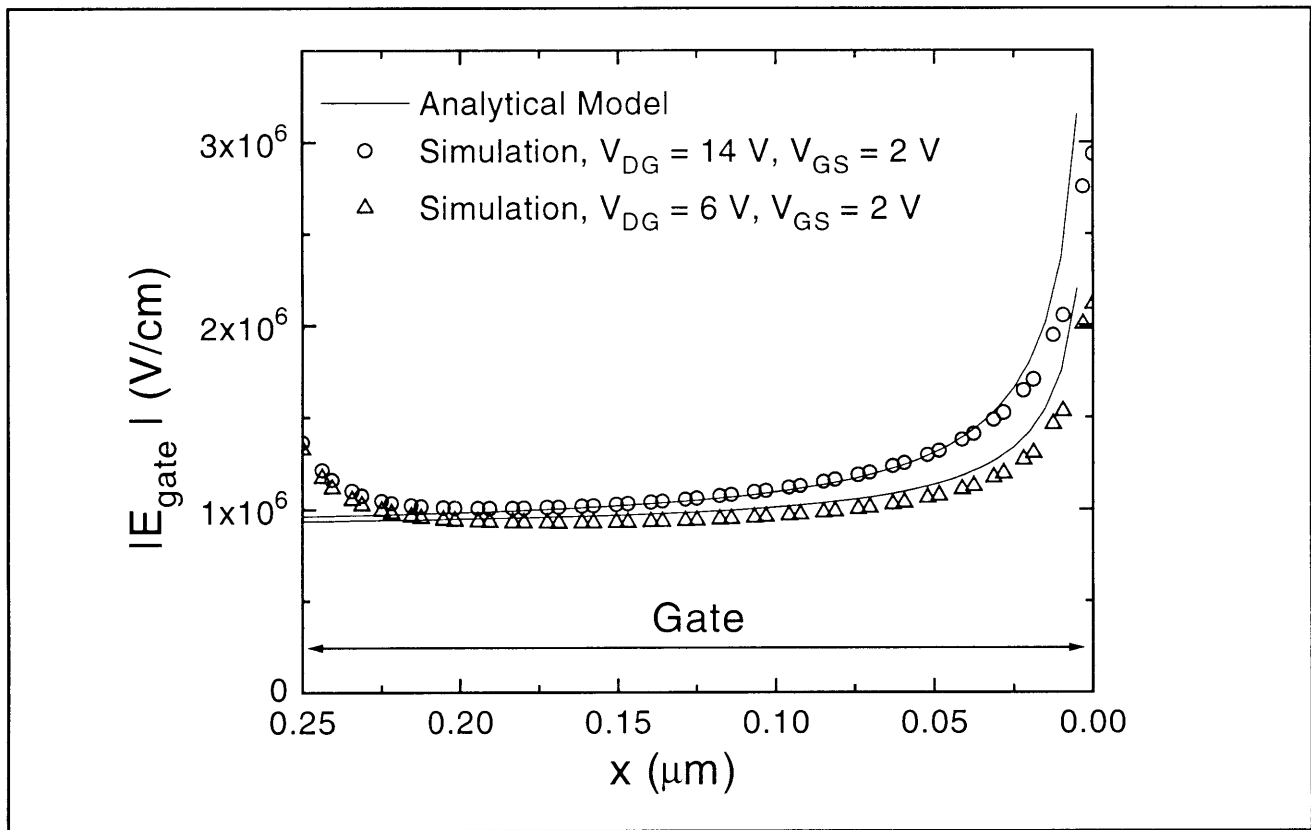


**Figure 4.** Comparison of simulated and calculated field profiles beneath the gate for two bias conditions. The model accurately captures the strong peak in electric field at the drain end of the gate.

**Table 1: Values of varied device parameters in 2D simulations. Note that all device parameters are centered about realistic values for state-of-the-art devices.**

Parameter	Simulated Values	Units
$t_{ins}$	180, 220, 27	Å
$t_{chan}$	130, 220, 300	Å
$L_G$	0.1, 0.25, 0.5	$\mu\text{m}$
$N_{tot}$	3, 4, 5	$10^{12} \text{ cm}^{-2}$
$N_{top}/N_{bot}$	3/2, 4/1, 5/0	-
$\Delta E_C$	0.3, 0.5	eV

As can be seen, the simplistic model we have proposed describes the shape of the field extremely well everywhere but at the source end of the gate, where the semi-infinite gate assumption becomes invalid. Simulations also show that our triangular description of the field in the channel is appropriate except in the immediate vicinity of the gate edge, where  $x' \approx t_{eff}$  (figure 5). The model accurately predicts the length of the depletion region under realistic bias conditions for a variety of  $n_{s(extr)}$  values

(figure 6); as can be seen,  $E_{gate(max)}$  depends linearly on  $x_D$ . Most importantly, the model yields the voltage-field relationship that is necessary to calculate the tunneling current (figure 7).

Examination of the leading terms in (2) and (3) makes it clear that the crucial parameter in determining breakdown due to tunneling is the carrier concentration in the extrinsic region. In order to explore this issue from a design perspective, we have performed a simple sensitivity analysis for the field beneath the gate at a given bias condition. A state-of-the-art device design was chosen as a baseline, and each design parameter of interest was individually varied to assess its impact on  $E_{gate}$ . All parameters were only varied within realistic boundaries for modern devices (values given in table 1). Our simulations clearly confirm the physical insight that for realistic designs,  $E_{gate(max)}$  the distribution of the field beneath the gate should depend strongly on  $n_{s(extr)}$  and should be independent of most other variables. Indeed, modifications to  $t_{chan}$ ,  $t_{ins}$ ,  $L_G$ , doping ratio  $N_{top}/N_{bot}$ , and  $\Delta E_C$  between insulator and channel had relatively little impact on  $E_{gate}$  so long as the total doping level ( $N_{tot}$ ) was held constant and the recess length on the drain was sufficient to accommodate  $x_D$  (figure 8). Our analysis establishes  $N_{tot}$ , which sets  $n_{s(extr)}$ ,

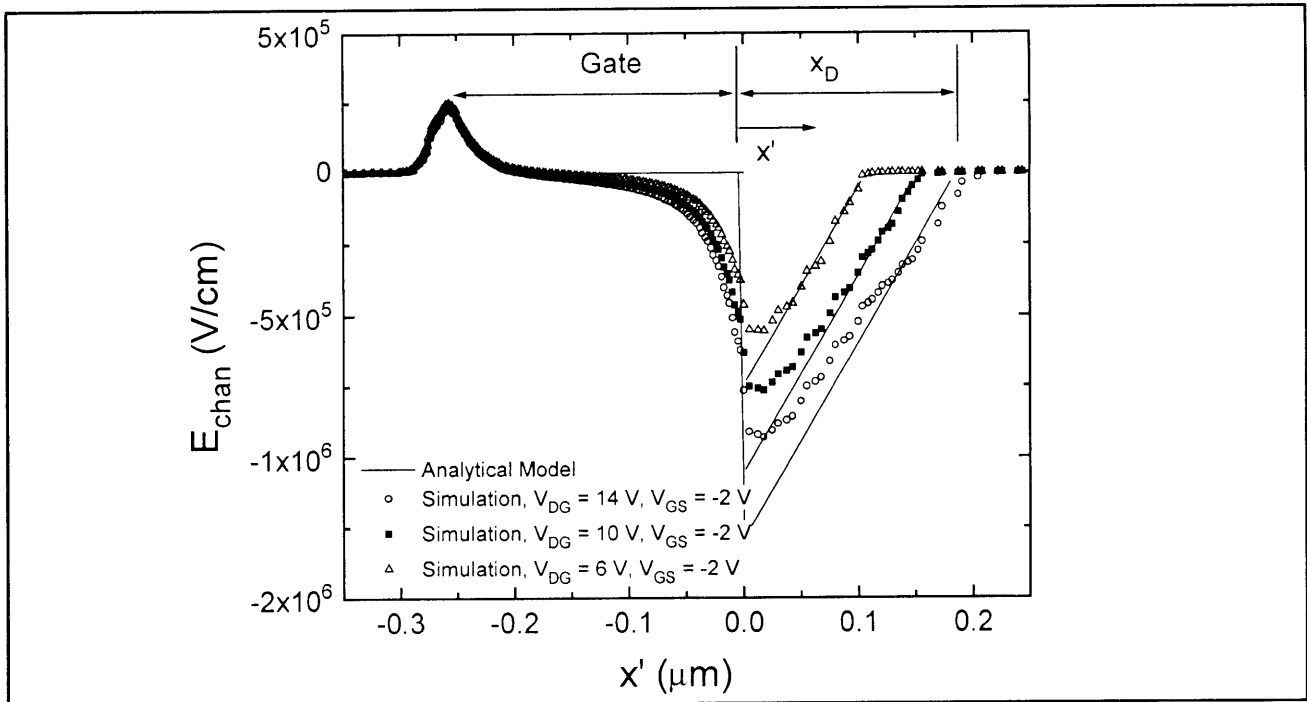


**Figure 5.** Simulated and calculated lateral field profile within the channel. For all values of  $V_{DG}$  the field displays a triangular behavior as demanded by the depletion approximation.

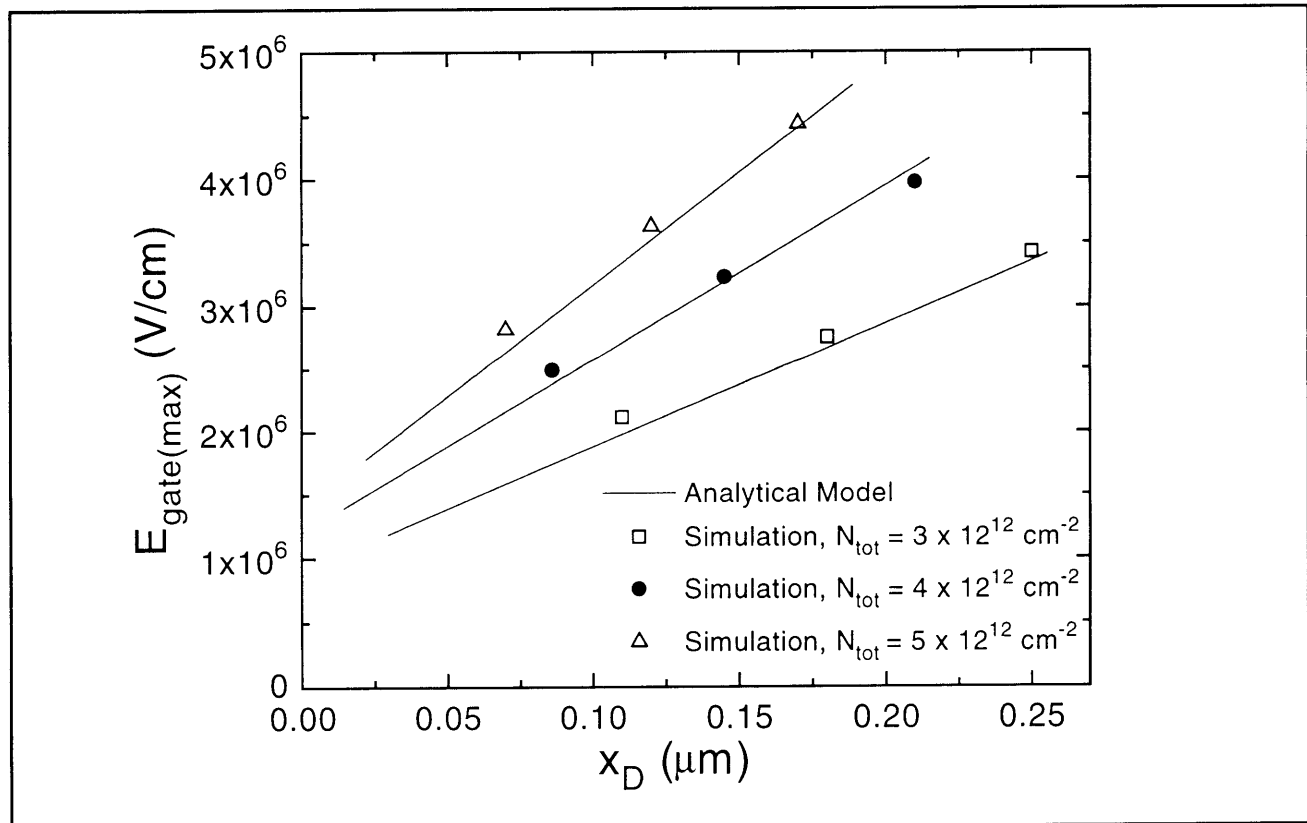


**Figure 6.** Simulated and calculated dependence of the maximum field at the drain end of the gate,  $E_{gate}(max)$ , on the length of the depletion region,  $x_D$ . The linear behavior indicates that the depletion charge is being imaged in accordance with the simple picture we propose ( $x_{min} = 70 \text{ \AA}$ ).

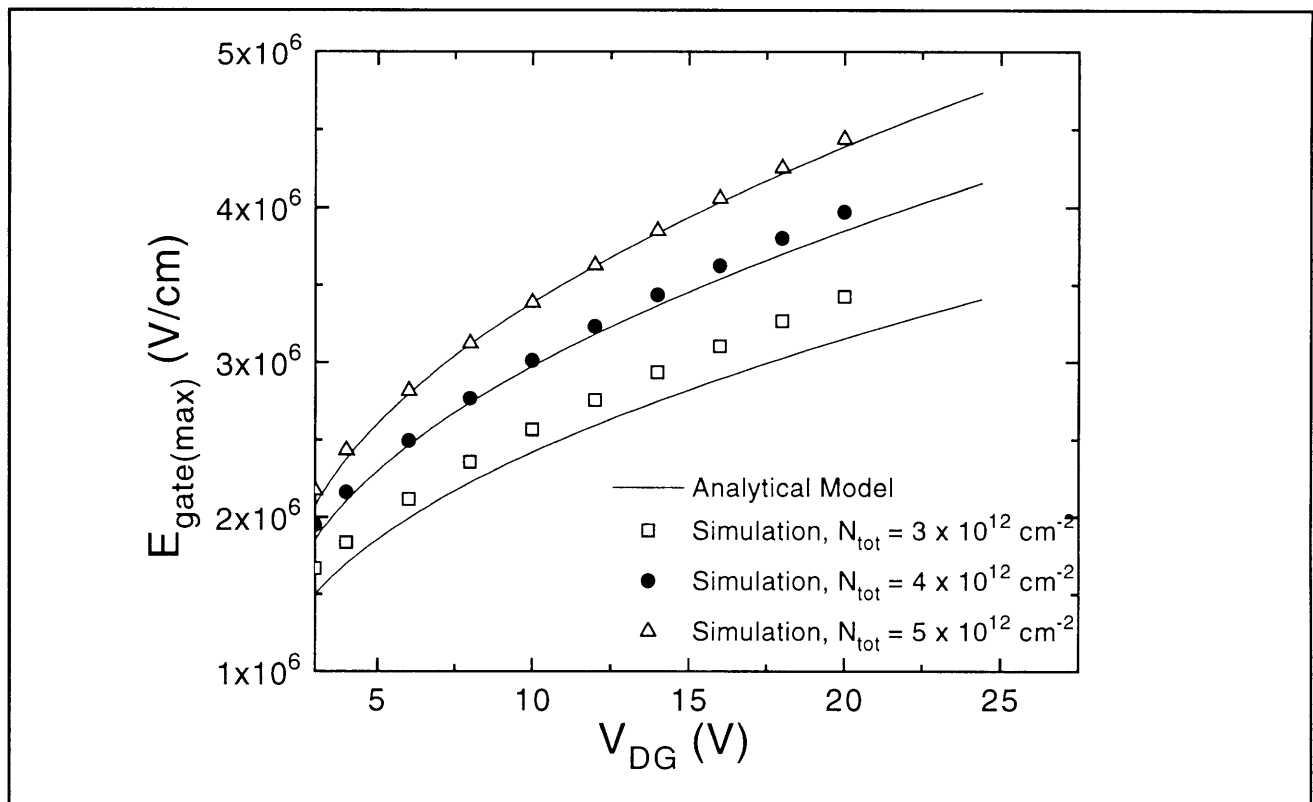


Figure 7.  $V_{\text{DG}}$  versus  $E_{\text{gate(max)}}$  from analytic model and 2D simulations ( $x_{\text{min}} = 70 \text{ \AA}$ ).

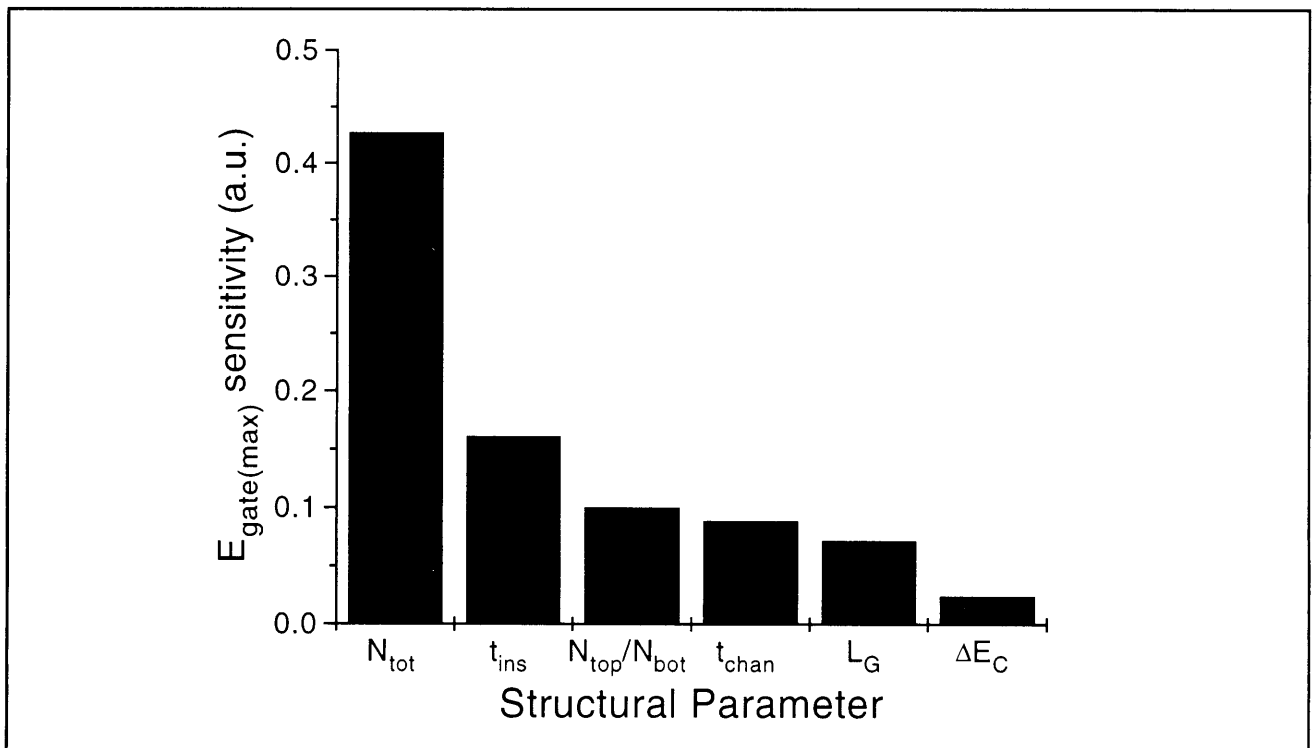
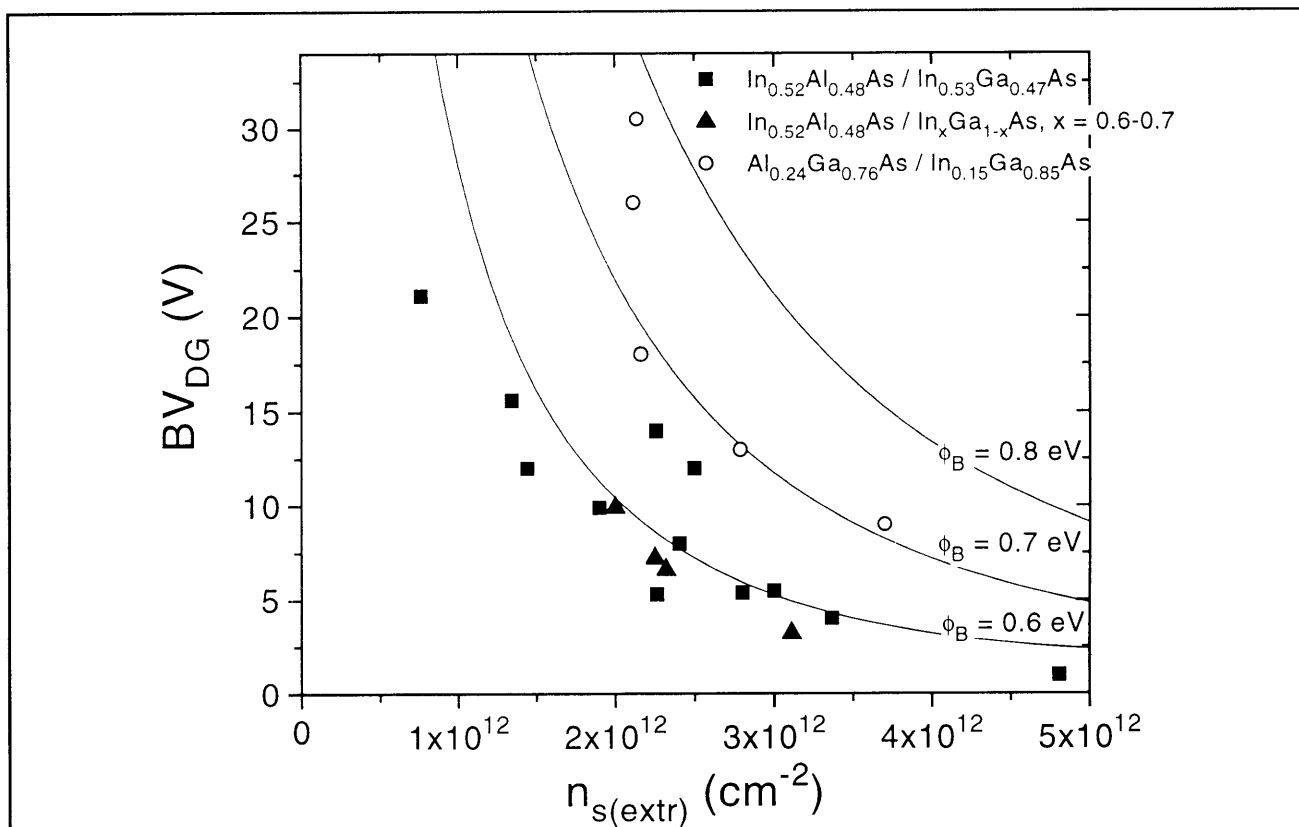


Figure 8. Sensitivity of maximum field beneath the gate to different structural parameters.  $N_{\text{tot}}$ , which establishes the sheet carrier concentration in the extrinsic region, emerges as the most critical structural parameter.





**Figure 9.** Predicted tunneling-limited breakdown voltage ( $I_G = 1$  mA/mm) as a function of extrinsic carrier concentration and barrier height. For non-selective recess technologies,  $n_{s(\text{extr})}$  is calculated based on  $I_{D\text{MAX}}$ . Note that InGaAs/InAlAs data obeys the expected trend regardless of indium content in the channel. The graph establishes the maximum attainable breakdown voltage for a given gate technology and extrinsic carrier concentration.

as the single most important parameter in determining  $E_{\text{gate}}$ .

Using our model, we can predict the tunneling current and the resulting BV limit in power HEMTs. Figure 9. plots the tunneling-limited BV as a function of  $n_{s(\text{extr})}$  and  $\phi_B$  (for  $I_G = 1$  mA/mm).<sup>16</sup> Also included in the figure are the results of several relatively well-controlled experiments varying  $n_{s(\text{extr})}$  in both the InAlAs/InGaAs system and in the AlGaAs/InGaAs system; as can be seen, the data behaves as the model predicts. Furthermore, the experiments indicate that the potential for improving BV without modifying  $n_{s(\text{extr})}$  or  $\phi_B$  appears to be limited.

Note that figure 9 includes both lattice-matched and strained channel data for the InAlAs/InGaAs system. The similarity between the strained and lattice-matched data is striking. This suggests the lower BV typically observed in high-indium channels is not due to enhanced impact ionization, but rather results from the increased  $n_{s(\text{extr})}$  usually achieved in such designs.

In summary, we have proposed a simple physical model for tunneling-limited off-state BV in HEMTs. Two critical parameters limit BV in power HEMTs:  $n_{s(\text{extr})}$  and  $\phi_B$ . Our model can also easily be extended to incorporate the additional reduction in BV arising from thermionic field emission.

<sup>16</sup> M.H. Somerville, J.A. del Alamo, and W.E. Hoke, "A New Physical Model for the Kink Effect on InAlAs/InGaAs HEMTs," *International Electronic Devices Meeting*, Washington, D.C., December 10-13, 1995; J.J. Brown, J.A. Puzl, M. Hu, A.E. Schmitz, D.P. Docter, J.B. Shealy, M.G. Case, M.A. Thompson, and L.D. Nguyen, "High-efficiency GaAs-based pHEMT C-band Power Amplifier," *IEEE Micro. Guided Wave Lett.* 6(2): 91 (1996); K.Y. Hur, R.A. McTaggart, B.W. LeBlanc, W.E. Hoke, A.B. Miller, T.E. Kazior, and L.M. Aucoin, "Double recessed AlInAs/GaInAs/InP HEMTs with High Breakdown Voltages," *IEEE GaAs IC Symp.*, 101 (1995); S.R. Bahl, *Physics and Technology of InAlAs/n-InGaAs Heterostructure Field-Effect Transistors*, Ph.D. diss., MIT Dept. of Elect. Eng. and Comput. Sci., MIT, 1993; H. Rohdin, A. Nagy, V. Robbins, C. Su, C. Madden, A. Wakita J. Raggio, and J. Seeger, "Low-Noise, High-Speed GaInAs/AlInAs 0.1  $\mu\text{m}$  MODFETs and High-gain/Bandwidth Three-stage Amplifier Fabricated on GaAs Substrate," *International Conference on InP and Related Materials*, Sapporo, Japan, 1995

### 2.3 Publications and Conference Papers

Somerville, M.H., J.A. del Alamo, and P. Saunier. "Off-State Breakdown in Power pHEMTs: the Impact of the Source," Fifty-fourth Device Research Conference, Santa Barbara, California, June 24-26, 1996.

Somerville, M.H., J.A. del Alamo, and W.E. Hoke. "Direct Correlation Between Impact Ionization and the Kink Effect in InAlAs/InGaAs HEMTs." *IEEE Electron. Device Lett.* 17 (10): 473-475 (1996).

Somerville, M.H., and J.A. del Alamo. "A Model for Tunneling-Limited Breakdown in High-Power HEMTs." *International Electronic Devices Meeting*, San Francisco, California, December 8-11, 1996, pp. 35-38.